A GRAPH-THEORETIC APPROACH TO BRAIN NETWORKS ASSOCIATED WITH SWALLOWING

by

Bo Luan

B.S. in Electrical Engineering, University of Pittsburgh, 2012

Submitted to the Graduate Faculty of

the Swanson School of Engineering in partial fulfillment

of the requirements for the degree of

Master of Science in Electrical Engineering

University of Pittsburgh

2013

UNIVERSITY OF PITTSBURGH

SWANSON SCHOOL OF ENGINEERING

This thesis was presented

by

Bo Luan

It was defended on

March 29, 2013

and approved by

Ervin Sejdić, Ph.D., Assistant Professor, Department of Electrical and Computer Engineering

Ching-Chung Li, Ph.D., Professor, Department of Electrical and Computer Engineering and Computer Science

Zhi-Hong Mao, Ph.D., Associate Professor, Department of Electrical and Computer Engineering and Bioengineering

Thesis Advisor: Ervin Sejdić, Ph.D., Assistant Professor, Department of Electrical and Computer Engineering

A GRAPH-THEORETIC APPROACH TO BRAIN NETWORKS ASSOCIATED WITH SWALLOWING

Bo Luan, M.S.

University of Pittsburgh, 2013

The functional connectivity between brain regions during swallowing is still not well understood. Understanding these complex interactions is of a great interest from scientific and clinical perspectives. In this study, we utilize functional magnetic resonance imaging (fMRI) to investigate brain functional networks during voluntary saliva swallowing in twenty two adult healthy subjects (all females, 23.1 ± 1.52 years of age). To construct these functional connections, we compute mean partial correlation matrices over ninety brain regions for each participant. Two regions are considered functionally connected if they showed statistically significant correlations. These correlation matrices are then analyzed using graph-theoretical approaches. In particular, we consider several network measures for the whole brain and swallowing-related brain regions. The results have shown that significant pairwise functional connections are mostly either local and intra-hemispheric or symmetrically inter-hemispheric. Furthermore, we have shown that the human brain functional network had robust small-world properties, which support efficient parallel information transfer at a relatively low cost. Swallowing related brain regions also had higher values for some of the network measures in comparison when these measures were calculated for the whole brain. Our results have demonstrated the basic network properties of the human brain compatible with previous functional network studies, but also showed unique connections in some regions during swallowing. This leads us to believe that graph-theoretical approaches are a valid tool for the analysis of the swallowing functional connectivity.

TABLE OF CONTENTS

LIST OF TABLES

LIST OF FIGURES

PREFACE

First and foremost, I would like to thank my parents and grandparents who blessed me with their enduring support, ceaseless encouragement and unconditional affection.

I would also like to thank my advisor Professor Ervin Sejdić for introducing me to this amazing field of brain connectivity and complex network analysis, as well as his support and guidance. I would also like to express my sincere appreciation to my committee members, Professor Ching-Chung Li and Professor Zhi-Hong Mao for their generous advice on improving this work, as well as broad guidance during my research and study.

I am also deeply appreciative to everyone that has encouraged and helped me during my research and study.

1.0 INTRODUCTION

1.1 SWALLOWING AND DIFFICULTIES ASSOCIATED WITH SWALLOWING

Human swallowing is also known as deglutition. It is a series of movements that are accomplished by the collaboration and coordination of multiple human biological systems and structures. Swallowing is a process in human or animals to pass material such as liquid, solid or compound that has already been broken into small pieces in the mouth and further to the pharynx. The material is subsequently transported into the esophagus while shutting the epiglottis, and further transfered into the digestive tract [1]. It is a complex neurological behavior which include the collaboration of multiple bodily structures near the mouth, as well as near the bilateral part of tongue, larynx, pharynx and esophagus [2], [3]. During a swallow, the epiglottis, a cartilaginous structure, shuts the entry towards the trachea to guarantee the material which has already been broken down in the mouth passes into the pharynx instead of entering the wrong tract, for example, entering the lungs [4], [5]. During the process, different part of the neuron system from the cerebral cortex are activated or excited sequentially to process the swallowed material from the mouth to the stomach [6], [7], [8], [9], [10] and [11]. The study of human swallowing behavior is challenging due to the complexity of the neurological structures, muscular organizations and nerve systems involved during the process of swallowing, which raised the difficulty but also the urgency of performing swallowing related experiments among human.

Dysphagia (swallowing difficulties) are usually the result of several known neurological conditions such as stroke, cerebral palsy, Parkinson's disease [12] or insults to motor or sensory pathways to the brain [13]. It is a serious and proemial condition due to its complication symptoms

such as degraded psycho-social well-being [14], dehydration, malnutrition [15] [16], acute stroke, acquired brain damage, and neuro-degenerative illnesses [17]. Patients with swallowing difficulties are vulnerable to the entry of foreign material into respiratory tract, as they will greatly increases the occurrence of severe respiratory problem among dysphagia patients. Therefore, understanding the neural basis of dysphagia is one of the paramount steps needed to develop future rehabilitation procedures.

Various diagnostic tool of dysphagia have been developed over past few decades, such as videofluoroscpotc swallowing study (VFSS) [18], [19]. Using VFSS approach, x-ray video record the activities of pharyngeal region during swallowing tasks of patients [18], [19]. The main purpose of utilizing VFSS approach is to asses the characteristic and seriousness of dysphagia and to come up with effective solution, if possible. However, due to the limitation of VFSS approach, such as cost and time frame required, many healthcare institutions are unable to provide VFSS [20]. Furthermore, VFSS is not a viable solution for long-term treatment of dysphagia due to heavy expense and tedious set-up procedures for every use. Because of the limitations of VFSS approach, researchers have proposed several alternative techniques. These techniques include pulse oximetry [21], cervical auscultation [22], and electro-physiological methods [23]. The above approaches employ non-invasive techniques. Among such alternatives, recent studies have demonstrated that the swallowing accelerometer performs as a cervical vibration evaluation device that essentially utilizes an accelerometer (e.g. [24], [25]). However, these studies also contains limitations. They are not able to automatically detect abnormal swallows due to the lack of using digital signal processing and pattern recognition techniques [24], [26]. Dual-axis swallowing accelerometry, which is the measurement of neck vibrations associated with deglutition, is another rising approach that can possibly evaluate the dysphagia condition. Compare to other methods, this approach is minimally invasive. It only requires the superficial attachment of a sensor anterior to the thyroid notch [27].

Swallowing is a complex activity that consist of multiple dynamic neuro-muscular and sensory motor movements. These movements originated from interacting cranial nerves of the brain stem and regulated by neural regulatory mechanisms in the medulla, sensorimotor, as well as limbic

cortical systems [5]. It has also been showed in the previous studies that dysphagia may be caused by a wide variety of neurologic diseases, and the largest proportion of patients with dysphagia have disorders localized to the oropharynx, and the most severe forms of dysphagia tend to affect the oropharynx [28]. Therefore, understanding the neural basis of dysphagia is essential to understand the mechanism of the disease.

1.2 HOW IMAGING STUDIES CAN HELP US UNDERSTAND SWALLOWING

Modern brain mapping techniques such as diffusion magnetic resonance imaging (dMRI), functional MRI, electroencephalography (EEG), and magnetoencephalography (MEG) produce high resolution and informative datasets consists of anatomical or functional connectivity profiles of human brain, which make the study of swallowing using neuroimaging approach become feasible.

The characterization of the topological structure of human brain functional networks is significant in the study of neuroscience. It would enlarge our perspective of how brain activities are in relation with the connection patterns between regions and provide new insight into the human neuron system. Various imaging techniques, although differ in terms of their data acquisition method, experimental setup and parcellation scheme, have allowed for non-invasive investigation of human brain networks. Via the acquired neuroimaging data (e.g. fMRI, EEG and MEG data), researchers have studied the functional brain networks (e.g., [29], [30], [31]) in humans and also demonstrated important properties of these networks, such as global efficiency (e.g., [32], [33]), characteristic path length (e.g., [34], [35]), as well as characteristics of these networks, such as small-world attributes (e.g., [33], [36]) and modularity (e.g., [37], [38]).

fMRI measures brain activity by detecting associated hemodynamic changes in blood flow [39]. fMRI is characterized by high spatial resolution, good availability in hospital facilities and the absence of radiating exposure [40]. One of the first studies employing graph theoretic approach with fMRI datasets measured the partial correlations relationship between 90 brain regions by acquiring resting-state blood oxygen level-dependent (BOLD) signals of 90 brain regions [41]. The whole-brain networks is constructed based on the partial correlation value between each of

the 90 brain regions. Small-world attributes are also discussed in this study. Other studies using fMRI imaging techniques have shown that functional and/or anatomically related brain regions have the tendency to be more densely interconnected compare to studies using other neuroimaging approaches (e.g., [37], [38]). Also, according to recent studies, the densely clustered connections between functionally connected regions increases the clustering coefficient value of the network, whereas the few number of long-range connections between different clusters keep the path length relatively low [36], [42], [41]. These studies all demonstrated that fMRI approach is likely to depict the neurological architecture of human brain at a more detailed level.

In the past few years, fMRI has shown tremendous advantage in the study of human brain. The stringency and consistency of the findings have established fMRI blood oxygenation level dependent signal imaging as a viable and powerful approach for studying brain activities in human. For example, fMRI acts as an effective tool to study the pathology of Parkinson's disease (PD). Structural and functional MRI provide an effective approach to investigate the cortical and subcortical regions that are likely to be related to PD. Structural MRIs allows visually asses symptoms in early-stage PD patients. The purpose of doing this is to eliminate the focus on irrelavant pathologies, including multiple sclerosis, tumors, vascular lesions, inflammation and atypical parkinsonian disorders [43]. fMRI also serve as a state biomarker of PD. The MRI technique has also been employed in the diagnosis of Alzheimer's disease (AD). AD is the most prevalent neurodegenerative disease [44] characterized by presence of amyloid aggregations and neurofibrillary tangles with a loss of cortical neurons and synapses [45], [46]. Cellular damage in specific cortical layers may disconnect hippocampal formation from the cerebral cortex [47], [48] and raise the possibility that functional interactions between the hippocampus and other related brain regions may be abnormal in the early stages of AD. Therefore, using fMRI technique, the AD could be diagnosed at early stage.

Similarly, fMRI studies have been used to understand the swallowing function. Recent neuroimaging studies have provided consistent evidence that swallowing is associated with activation in multiple regions of the human brain [49], [50], [51], [52], [53], [54], [55], [56], [57]. Prior analysis of brain functions during swallowing revealed activation clusters exist in the supplemen-

tary motor area, anterior cingulate and paracingulate gyri, pre- and postcentral gyrus [58]. Several other regions have also been found related to swallowing, including the posterior insula [59], basal ganglia, thalamus, and cerebellum. Despite these findings, interactions between different swallowing-related brain regions are still not well understood.

1.3 MOTIVATION AND SIGNIFICANCE OF THE WORK

Functional networks study demonstrates the neurophysiological organization of the human brain that is large-scale, robust, interactive and characterized by various network properties, such as optimal small-world properties [36], [60]. The brain is considered to be one of the most challenging networks found in nature [35]. This biological system responds to any external stimulus by transporting signals between specialized brain regions. Therefore, the study of brain functional connectivity contributes greatly to the understanding of brain functions and pathology.

Previous studies on graph theory suggested the possibility of performing network analysis on human brain [36]. Via network analysis, the large variability of the brain structure could be abstractly reduced to a collection of nodes and links (edges). For functional networks, nodes stand for brain regions and links stand for connections in between. By graph theoretic approach, the differences and similarities in the structure of brain functional networks can be easily identified. Also, the brain network shows consistent topology so that properties, such as small-worldness, could generally be identified in all human brain networks [61]. Furthermore, given that network nodes stand for brain regions and links stand for connections in between, comparison between different kinds of networks become fairly feasible [61].

The goal of this thesis was to demonstrate how the use of graph-theoretic approaches can characterize the interaction between brain regions during voluntary saliva swallowing in healthy young adults.

1.4 CONTRIBUTION OF THIS THESIS

In this thesis, we consider several network measures for the whole brain and swallowing-related brain regions. The results have shown that significant pairwise functional connections are mostly either local and intra-hemispheric or symmetrically inter-hemispheric. Furthermore, we have shown that the human brain functional network have robust small-world properties, which supports efficient parallel information transfer at a relatively low cost. Swallowing related brain regions also have higher values for some of the network measures in comparison when these measures are calculated for the whole brain. Our results have demonstrated the basic network properties of the human brain compatible with previous functional network studies, but have also shown unique connections in some regions during swallowing. This leads us to believe that graph-theoretical approaches are a valid tool for the understanding the neural basis of swallowing.

1.5 THESIS STRUCTURE

In Chapter 2 the fundamental of swallowing, swallowing difficulties, graph theory and brain networks will be illustrated. Chapter 3 will introduce the experiment setup, data preprocessing approach and techniques. Mathematical expressions for the complex network analysis will be discussed in detail as well as construction of functional connectivity networks. The results including the connectivity matrix we constructed and network parameters calculated will be presented in Chapter 4. The conclusion and future work will be indicated in Chapter 5.

2.0 BACKGROUND

2.1 SWALLOWING IN HUMANS

Swallowing is a process for human or animals to pass food or drink that has been broken down in the mouth into the pharynx, commonly known as throat, and subsequently into the esophagus, so that it may be further pushed through the digestive tract. During swallowing movements, a cartilaginous structure called epiglottis closes over the pharynx entrance to the trachea. This ensures that the swallowed material passes into the pharynx behind it instead of getting the material into the lungs. This process is a reflex that prevent a person from choking. Furthermore, the swallowing reflex also prevents food from entering the wrong tract, such as pulmonary aspiration [62]. A anatomical view of mouth and pharynx can be seen in Figure 2.1.

Swallowing is known scientifically as deglutition. It is a complex physiological process which involves voluntary and reflexive motor activity, sensorimotor integration, salivation, and visceral regulation [57]. Swallowing requires the coordination of several human body systems and structures. To be specific, swallowing can be subdivided into several distinct stages: oral, pharyngeal, and esophageal [63]. Each stage involves a different control center in the central or peripheral nervous system. The first oral phase is often considered as voluntary. This phase is highly variable in duration because of variation in taste of materials swallowed, environment, hunger, motivation, as well as consciousness for the human subject [57]. The oral phase consists of movement of tongue. During the phase saliva releases and chemically breakdown the food as well as moisturize it, initiate the movement of bolus to and moves the broken down and moistened food to the back of the mouth [2]. This phase is purely voluntary, which indicates it is done completely by skeletal

muscles, those that facilitate conscious movement [63]. Therefore, the oral phase is managed by the limbic system in the central nervous system, the medial temporal lobes, and other involving brain structures in the cerebral cortex [57]. The oral phase is ended by the activation of next phase of the swallowing, which is the pharyngeal phase. Compare to the oral phase, the rest two phases

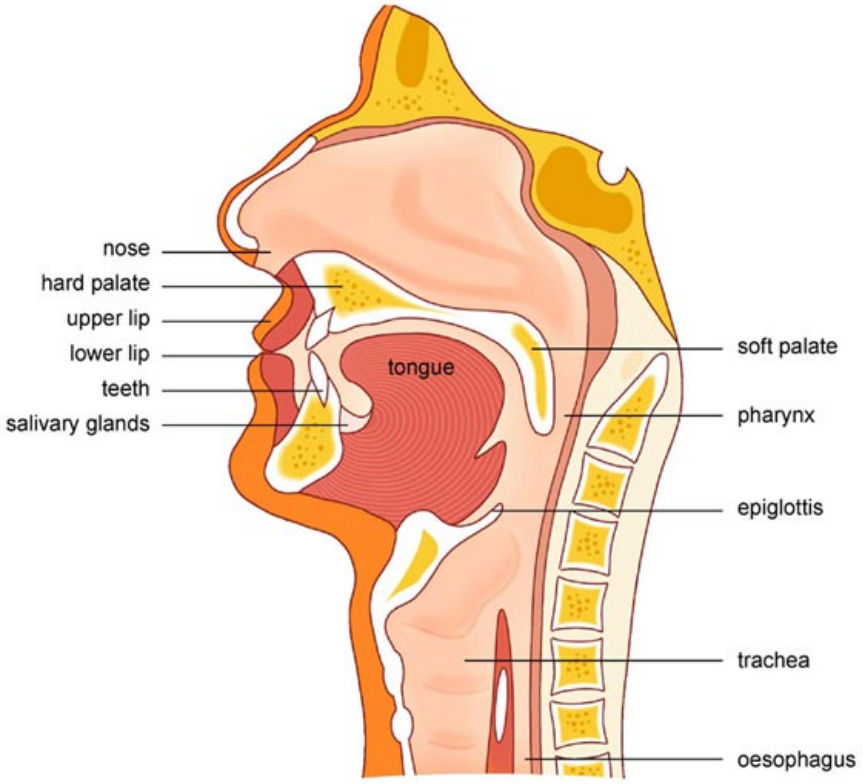

Figure 2.1: Anatomy of a swallowing process. This figure is adopted from [64].

are involuntary. They controlled by the autonomic nervous system, the part of the peripheral nervous system which performs the functions like heart activities, breathing, and digestion [57]. The second phase pharyngeal phase is considered a reflex response. During this phase, the broken down material has been pushed to the pharynx. In order of this movement to happen, other tracts to pharynx must be temporarily closed as the pharynx becomes triggered by small skeletal muscles in order to prepare the entry of the swallowed material [2].

The third phase of swallowing started when the involuntary smooth muscle contractions within the pharynx have pushed the bolus into the esophagus. Esophageal phase is primarily under dual control of the somatic and autonomic nervous systems [65], [66], [63], [4]. The food transfered to stomach during the esophageal phase without any interruption. The movement is initially motivated by esophagus via skeletal muscle and then by smooth muscle, which moves the swallowed material during peristalsis process [2].

2.2 GRAPH THEORY AND BRAIN NETWORKS

A large number of biological system can be abstractly represented by complex networks [67]. Graph theory is generally considered to be the most viable platform for the mathematical analysis of complex networks. Originated in the field of mathematics, graph theory is the study of graphs. Graph, in the field of study of functional connectivity, is a collection of nodes and links shown in Figure 2.2. Graph theory has shown its tremendous advantage when dealing with real-world system. A graph represents the complex structure of human brain in a simplified manner using nodes and links. For example, the nodes in human brain network ideally represent brain regions with coherent pattern of extrinsic functional connections, while links represent connections in between brain regions [61], [68].

The characteristic of nodes and links in human brain networks is determined by combinations of brain imaging technique, anatomical parcellation schemes, pre-processing approach and measurement scale of connectivity. Many combinations occur in various experimental settings [69]. The choice of the nodes, therefore, must be carefully determined as it may influence the network properties greatly [67]. Base on this fact, the network can only be compared if they used the same preprocessing approach. fMRI techniques, in this regard, shows its advantage compare to EEG and MEG techniques, since the limitations of EEG and MEG makes the sensors may detect spatially overlapping signals and are generally not aligned with boundaries of coherent regions [68], [70].

Links can be differentiated by their directionality and weight [61]. It can be either directed, meaning that there is distinction between the two nodes, or it can be undirected, meaning that there

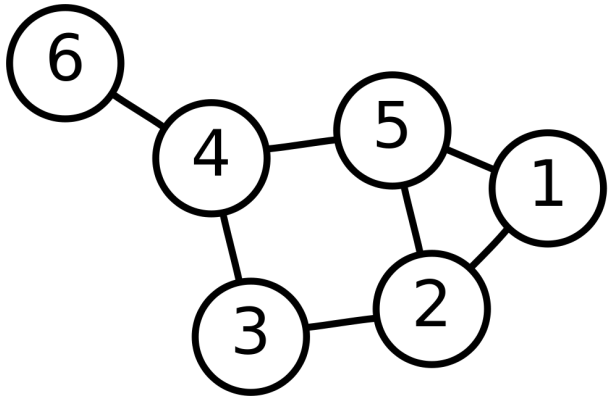

Figure 2.2: A drawing of a labeled graph on 6 vertices and 7 edges. This figure is adopted from [71].

is no distinction between two nodes. Sample links are depicted in Figure 2.2. Furthermore, links can be binarized or weighted. Binary links denote the absence or presence of connection between two vertices, while weighted links also indicate the connectivity strength between nodes [68]. In structural connectivity networks, connection weights may indicate amount of fibers, likelihood of connection, or the amount of dye traverse between two nodes while in functional connectivity study weights indicate the correlation of time series between brain regions [61], [67]. Weights in anatomical networks may represent the density of anatomical connections, while weights in functional and effective networks may represent magnitudes of correlational or causal connections [68]. For functional connectivity, weighted links can represent the connectivity strength between different nodes. For effective connectivity, weighted links suggest a causal relationships between two nodes. Based on these nature of the links, we further divide the network to binary directed network (BD), binary undirected network (BU), weighted directed network (WD) and weighted undirected (WU) network. Figure 2.3 depicts sample networks. Weighted networks and binary networks can be converted to each other using a sparsity threshold so that connections are established only if the weight is above a certain threshold level. A lot of connectivity studies tends to construct binary network as compare to weighted network, binary network are easier to characterize.

In weighted network, weak links may represent non-significant connections or even spurious connections. This is particularly evident in functional or effective networks. A lot of weak links have the tendency to attenuate the pattern of strong and significant connections and as a result are discarded. This process is done by applying an absolute, or a proportional weight threshold to the network. Threshold values are often arbitrarily determined through a broad range of selection. Furthermore, all self-connections or negative connections (such as functional anti-correlations) must currently be removed from the networks prior to analysis [68].

Functional connectivity networks reflect how brain regions are connected by functional associations. Graph theory analysis - a new multidisciplinary approach to the study of neuroimaging research - provides simplification to the interactions between brain regions [68]. The human brain shows a large variability in size and surface shape. Complex network analysis, by reducing the complexity of these properties, can help to identify the similarities and differences in the organization of neural networks [61]. Also, the comparison within and between subjects becomes feasible. The basic elements of network analysis, such as nodes and links, correspond to the connectivity profiles of the system and therefore reflect the way the elements are placed in the network [68]. Many brain network studies investigate brain's topological properties by simplifying weighted and directed variants of measures to binary graphs so that every appearance of the connection has equal value of one [61], [30], [72], [29].

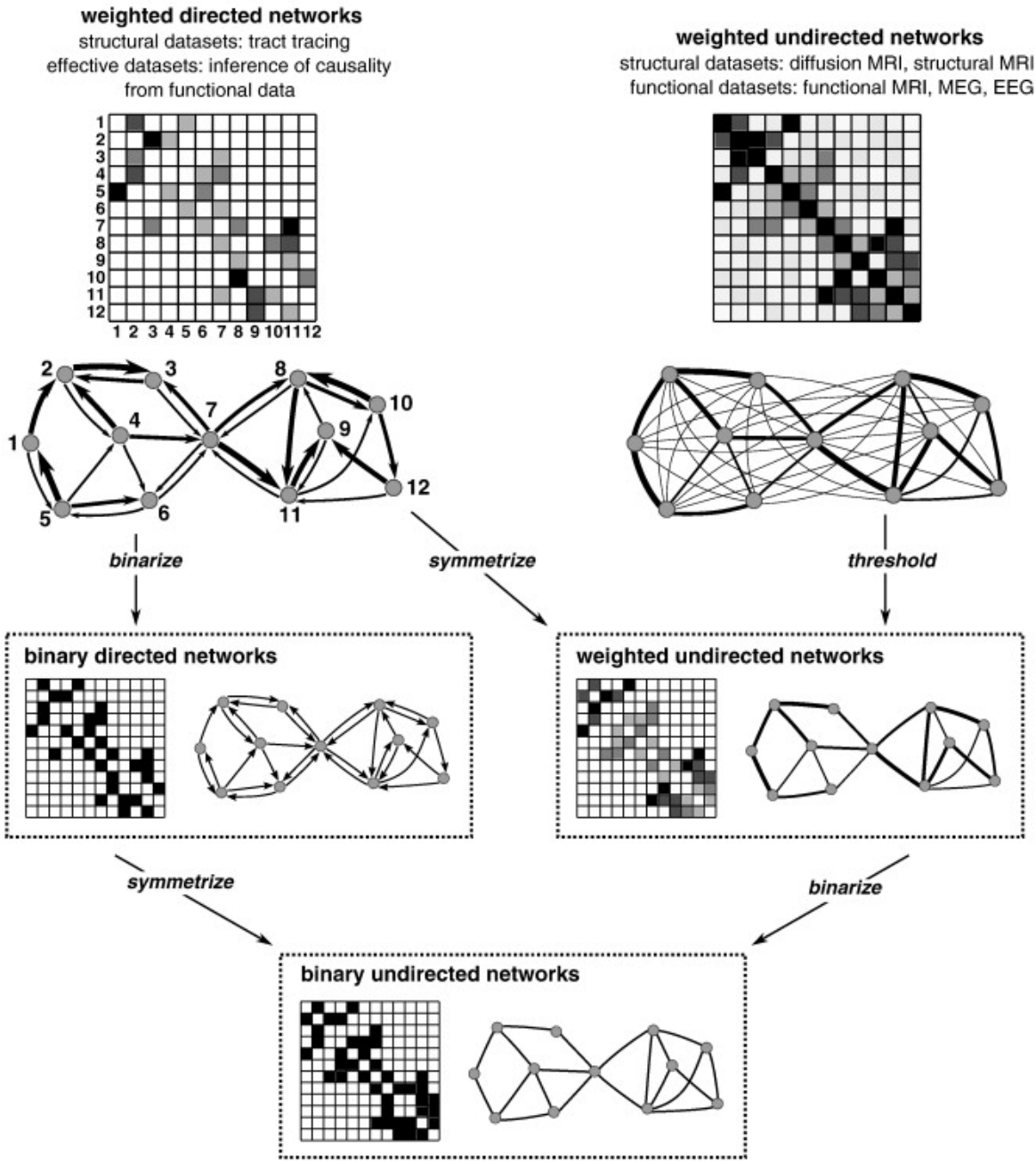

Figure 2.3: Construction of brain networks from large scale anatomical and functional connectivity datasets. This figure is adopted from [68].

3.0 THEORIES AND METHODS

3.1 DATA ACQUISITION

Twenty-two healthy young-adult subjects, all females (23.1 ± 1.52 years), participated in this study after providing written, informed consent. The study protocol was approved by the University of South Carolina Institutional Review Board.

All functional magnetic resonance scans of the brain were acquired on a Siemens Magnetom Tesla Trio Tim scanner with a 32-channel RF-receive head coil at the McCausland Center for Brain Imaging, University of South Carolina, Columbia, SC, USA. These blood oxygen level dependent (BOLD) images were acquired using an echo planar imaging sequence in 36 axial slices (TR = 2200 ms, TE = 35 ms, flip angle = 90°, FOV = 192 mm; 3 mm thickness) during swallowing. During our experiment, participants were instructed to swallow their accumulated saliva every 44 seconds (every 20 volumes acquired). They were directed to move as little as possible. They were also instructed not to produce exaggerated oral movements to increase or manipulate the accumulation of saliva. The saliva should be accumulated passively prior to swallowing. A comfortable custom-built restraint was applied during fMRI scans to minimize head movement. A high-resolution T1-weighted MRI sequence was also performed during the data collection (3D MP-RAGE, 176 axial slices with 1 mm slice thickness, a 256×256 matrix, and 256 mm $\times$ 256 mm FOV).

3.2 DATA PREPROCESSING STEPS

3.2.1 fMRI Data Preprocessing

All data in the study were preprocessed using statistical parametric mapping (SPM) software [73]. For each subject 350 volumes of the scans were acquired, and the beginning 10 scans were discarded for magnetic equilibrium. The remaining each of the 340 volumes underwent the following four preprocessing steps accordingly: realignment, coregistration, normalization and smoothing. Excess motion defined as greater than 4.0 mm of translation/rotation was eliminated in any of the task-free scans.

Specifically, the fMRI scans for each subject were first adjusted for time delay between different scans. Second, for each subject the images were realigned to the first slices among all slices using a least squares fitting algorithm and a 6 parameter rigid body transformation [74] to correct for head motion. The following formula for head movement calculates the group difference in translation and rotation [33]:

$$Headmotion/Rotation = \frac{1}{M-1}\sum_{i=2}^{M}\sqrt{|x_i - x_{i-1}|^2 + |y_i - y_{i-1}|^2 + |z_i - z_{i-1}|^2} \tag{3.1}$$

where $M = 340$ represents the length of the time series. The x_i, y_i and z_i are the translations or rotations magnitude in the x, y and z directions at $i-th$ time point, respectively.

After removing the movement artifact in fMRI images, the fMRI images further underwent the coregistration step during which the mean fMRI scans were overlayed to a high resolution anatomical image to maximize the mutual information. Therefore, all other functional images were resliced to align with the reference image.

Then, to make inter-individual comparisons, normalization was then performed to warp the images to fit a standard MNI (Montreal Neurological Institute) template. Finally, smoothing was applied with Gaussian kernel with a 4-mm full-width at half maximum to suppress noise and effects due to residual differences [73].

3.2.2 Anatomic Parcellation

The choice of nodes and links greatly influences the results of network connectivity analysis [68]. We chose the parcellation (segmentation) scheme that has been used previously in many studies (e.g., [30], [33], [41], [75]). Therefore, the preprocessed fMRI datasets were parcellated into 116 anatomical ROIs via the automated anatomical labeling (AAL) template [76]. The AAL parcellation scheme segments the cerebrum into 90 cortical and subcortical anatomical ROIs (45 ROIs in each hemisphere) [76]. It divides the cerebellum into 26 ROIs (8 in the vermis and 18 in cerebellar hemisphere, 9 in each side of cerebellar hemisphere). This study considered the 90 cerebrum regions summarized in Table 3.1. This parcellation scheme provides non-overlapping segmentation of the entire brain volume such that each brain area depicted in AAL only points to one brain region in Table 3.1. These individual anatomical ROIs were parcellated from whole brain by the MarsBaR toolbox [77]. Therefore, for each subject, we generated 90 time series for all the 90 anatomical ROIs in Table 3.1. The mean time series is the average of voxels for every time point in the time series over all 22 subjects in the study. This procedure generated the mean time-series with 340 time points. These 90 mean time series were then correlated with each other to establish a 90×90 brain functional connectivity matrix.

3.3 COMPLEX NETWORK ANALYSIS

A graph theory definition of a network is that it is a collection of sets of nodes and links, where a node is considered as the most essential element of the network [68]. A graph theory based approach can quantitatively and analytically depict a wide variety of measures for brain networks. However, various measurement can describe a network in an effective way. Therefore, only some of the measurements that were used in previous connectivity studies are discussed here.

For binary undirected networks, we use a_{ij} to represent the connection status in the network between node i and j. $a_{ij} = 0$ when no connection exists between two nodes and $a_{ij} = 1$ when the connection is present between two nodes. For weighted undirected networks, w_{ij} is the connection

Table 3.1: Cortical and sub-cortical regions (45 in each cerebral hemisphere; 90 in total) as anatomically defined in the AAL template and their corresponding abbreviations used in this study.

Region	Abbreviation	Region	Abbreviation
Precentral gyrus	PreCG	Supramarginal gyrus	SMG
Postcentral gyrus	PosCG	Precuneus	PCUN
Rolandic operculum	ROL	Superior occipital gyrus	SOG
Superior frontal gyrus, dorsolateral	SFGdor	Middle occipital gyrus	MOG
Middle frontal gyrus	MFG	Inferior occipital gyrus	IOG
Inferior frontal gyrus, opercular part	IFGoper	Cuneus	CUN
Inferior frontal gyrus, triangular part	IFGtri	Calcarine fissure and surrounding cortex	CAL
Superior frontal gyrus, medial	SFGmed	Lingual gyrus	LING
Supplementary motor area	SMA	Fusiform gyrus	FFG
Paracentral lobule	PCL	Temporal pole: superior temporal gyrus	TPOstg
Superior frontal gyrus, orbital part	SFGorb	Temporal pole: middle temporal gyrus	TPO
Superior frontal gyrus, medial orbital	SFGmedorb	Anterior cingulate and paracingulate gyri	ACP
Middle frontal gyrus, orbital part	MFGorb	Median cingulate and paracingulate gyri	MCP
Inferior frontal gyrus, orbital part	IFGorb	Posterior cingulate gyrus	PCG
Gyrus rectus	GRE	Hippocampus	HIP
Olfactory cortex	OLF	Parahippocampal gyrus	PHG
Superior temporal gyrus	STG	Insula	INS
Heschl gyrus	HES	Amygdala	AMY
Middle temporal gyrus	MTG	Caudate nucleus	CAU
Inferior temporal gyrus	ITG	Lenticular nucleus, putamen	PUT
Superior parietal gyrus	SPG	Lenticular nucleus, pallidum	PAL
Inferior parietal, but supramarginal and angular gyri	IPL	Thalamus	THA
Angular gyrus	ANG		

between nodes i and j, and it has range $0 < w_{ij} < 1$. Because of the limitation of current fMRI neuroimaging technique, the weighted directed network cannot be constructed in this study.

Node degree The node degree describes the number of direct connections a node has with the rest of the nodes in the network. The node degree is considered to be the most fundamental network measure. It is also a foundation for most of the network measures in this study. The summation of all the node degrees in a set in the network derives a degree distribution [67]. In a random network, connections are distributed randomly and uniformly with a symmetrical Gaussian shape and centered degree distribution [78]. A brain functional network, however, has a non-Gaussian distribution with a tendency to spread towards higher degrees [67]. Thus, we later introduce the rank-sum test to discuss the difference between two different groups.

The degree D_i of a node i is the number of nodes directly connected to the *ith* node. For a binary network, the node degree is defined as $k_i = \sum_{j \in N} a_{ij}$ and for a weighted network it is defined as $k_i = \sum_{j \in N} w_{ij}$, where N is the set of all nodes in a collection, and n is the number of nodes in the collection. Given that whole-brain was parcellated into 90 ROIs, therefore, n is equal to 90, and N is the set of different possibilities (e.g., $N \in \{1,2,3...90\}$. The degree of the entire network, therefore, is calculated by averaging all the nodes in the network:

$$D = \frac{1}{n} \sum_{i \in N} D_i. \tag{3.2}$$

Clustering Coefficient The clustering coefficient C_i of a node i calculates the ratio between the number of existing connections and the maximum number of connections in a set of nodes [34]. The existing connections here are defined as the links between the direct neighbors of the node i. Connections in random networks are uniformly and randomly distributed so that clustering coefficient are relatively low for a random network, whereas complex networks contain densely connected clusters leading to a higher clustering coefficient [78]. For a binary network, the clustering coefficient C_i^B of the node i is calculated as [72]:

$$C_i^B = \frac{E_i}{D_i(D_i - 1)/2} \tag{3.3}$$

in which E_i is the number of links in *ith* set of nodes N_i ($N_i \subset N$), and D_i is the degree of node i mentioned above. The clustering coefficient C_i^W of a node i in a weighted network is calculated as [72]:

$$C_i^W = \frac{1}{S_i(D_i-1)} \sum_{j,h} \frac{w_{ij}+w_{ih}}{2} a_{ij}a_{ih}a_{jh} \tag{3.4}$$

where the normalizing factor $S_i(D_i-1)$ assures that $0 \leq C_i^W \leq 1$; $S_i = \sum_{j=1}^{N} a_{ij}w_{ij}$; D_i is the degree of a node i. a_{ij} is the connection status between node i and node j. The value of a_{ij} is 1 if there is an link connecting node i and node j, and it is equal to 0 if no connection is presented. This applies to a_{ih} and a_{jh} as well. Therefore, the clustering coefficient of a n-nodes network is calculated as [68]:

$$C = \frac{1}{n} \sum_{i \in N} C_i \tag{3.5}$$

where $C_i = C_i^B$ for binary networks and $C_i = C_i^W$ for weighted networks.

Path Length The shortest path length L_i is given by the shortest distance to go from the node i to another node. The shortest path between two nodes could consist of multiple connections in between when there is no direct connection between them. In comparison to regular networks, complex and random networks generally have short path lengths [67]. The definition of complex, random and regular networks can be found in [36]. The mean path length for a node i is defined as [68]:

$$L_i = \frac{1}{n-1} \sum_{i,j \in N, i \neq j} d_{ij} \tag{3.6}$$

where d_{ij} is the shortest distance between node i and node j. In a binary network, the value of every existing link is 1. d_{ij} is thus the number of links connecting node i and node j. However, for a weighted network, the shortest path length is not necessarily the optimal value, as the weighted network also contain information about connection strength (thickness of link) between nodes [68]. To differentiate the strength of these connections in weighted network, the strength of every link between node i and node j is associated with weight indices w_{ij}. This weight indices value was normalized to a range from 0 to 1 [72].

To calculate the weight indices in weighted network, we followed the approach given by Boccaletti et al. [79]. Let the length between nodes i and j inversely proportional to the weight indices w_{ij}:

$$l_{ij} = \frac{1}{w_{ij}} \tag{3.7}$$

For the weighted network, $d_{ij} = l_{ij}$. Then the mean shortest absolute path length of the network is the average of shortest absolute path length of all nodes [68]:

$$L = \frac{1}{n} \sum_{i \in N} L_i \tag{3.8}$$

Global Efficiency The global efficiency of a network, E_{glob}, measures the average inverse shortest path length [80]. It is inversely related to the characteristic path length, and is an alternative way to indicate the parallel information transfer efficiency in the network [36], [81]. It is an alternative way to describe the connectivity of the network [81], [82]. In comparison to the characteristic path length, the global efficiency makes quantifying disconnected networks possible[68]. Mathematically, for both binary and weighted functional networks, the global efficiency for a node i is calculated as [72]:

$$E_{glob,i} = \frac{1}{n-1} \sum_{i,j \in N, i \neq j} d_{ij}^{-1}. \tag{3.9}$$

In comparison to the path length (eqn. 3.6), the global efficiency of a node i calculates the inverse of the harmonic mean of the minimum absolute path length between node i and others [81]. The global efficiency of the network is the average of global efficiency for all nodes and is calculated as:

$$E_{glob} = \frac{1}{n} \sum_{i \in N} E_{glob,i} \tag{3.10}$$

Local Efficiency For binary networks, the local efficiency of the $i-th$ node is calculated as:

$$E^B_{loc,i} = \frac{1}{D_i(D_i-1)} \sum_{j,h \in N, i \neq j} a_{ij} a_{ih} [d_{jh}(N_i)]^{-1} \tag{3.11}$$

where $d_{jh}(N_i)$ is the shortest path length between j and h that contains only neighbors of i. For weighted networks, the local efficiency of the node i is defined as:

$$E^W_{loc,i} = \frac{1}{D_i(D_i-1)} \sum_{j,h \in N, i \neq j} (w_{ij} w_{ih} [d^w_{jh}(N_i)]^{-1})^{1/3} \tag{3.12}$$

3.3.1 Analysis of Whole-Brain Network Small-World Attribute

Small-world measurements (e.g., [36]) involve a mean cluster coefficient C and a mean characteristic path length L. To be specific, the parameter C is the average of the clustering coefficient over all nodes in the functional network. It quantifies the level of cliquishness (local interconnectivity) of a typical neighborhood [36]. The parameter L of a network is reflected by harmonic mean distance between pairs proposed by [83], which is defined as the reciprocal of the average of the reciprocals:

$$L^{-1} = \frac{1}{\frac{1}{2}n(n+1)} \sum_{i \geq j} d_{ij}^{-1} \tag{3.13}$$

A high clustering coefficient and a short characteristic path length suggests the network is described by optimal small-world attributes [36], [82], [84]. In other words, a network has less than optimal organization if the absolute path length is relatively short and the absolute clustering coefficient is relatively low [33]. Mathematically, a network would be classified as a small-world network if it satisfies the following two conditions [60]:

$$\gamma = \frac{C}{C_{rand}} \gg 1 \tag{3.14}$$

and

$$\lambda = \frac{L}{L_{rand}} \approx 1 \tag{3.15}$$

in which C_{rand} indicates the mean clustering coefficient of a random network and L_{rand} indicates the mean characteristic path length of a random network. The random network preserves the same amount of nodes, links and degree distribution as the functional network. The C_{rand} and L_{rand} values are calculated by generating many random networks for each individual's functional network. Note that the small-worldness parameter might vary with the change of the sparsity threshold value. When a more rigorous sparsity threshold is chosen, fewer connections will likely to exist, leading to a sparser network [85]. Mathematically, the small-worldness is calculated as:

$$S = \frac{C/C_{rand}}{L/L_{rand}} \tag{3.16}$$

3.3.2 Analysis of Whole-Brain Network Hierarchy

In addition to small-world attribute, the hierarchy is used to characterize topological properties of human brain [86], as it offers an alternative view on the topological properties of complex networks [87]. The hierarchy of the networks was interpreted by the coefficient β, which describes the relationship between clustering coefficient C and node degree k of the network [87] using a power law approach: $C \sim k^{-\beta}$. Networks with a high hierarchy value are characterized by a higher degree k and low clustering coefficient C, and vice versa. The networks with hierarchical structures contain interconnected clusters, which are the combination of smaller and more densely connected clusters [87].

3.4 CONSTRUCTION OF FUNCTIONAL CONNECTIVITY NETWORKS

Functional connectivity networks share various significant common ground with anatomical and structural connectivity networks [88], but they also have obvious differences. For example, in structural connectivity networks, connection weights indicate amount of fibers between regions, the degree of myelination, the probability of connection between two nodes, or the amount of dye traverse between two nodes while in functional connectivity study weights indicate the correlation in the time course of signals of different nodes [61].

Partial correlation could measure the inter-regional functional connectivity by attenuating the contribution of other sources of covariance [89]. A partial correlation matrix is a symmetrical matrix derived from fMRI time series of each participant. In the correlation matrix, each off-diagonal entry is the correlation between a pair of variables (brain regions) while attenuating their correlation with other variables [33]. In this case, given 90 regions defined in the study in Table 3.1, a symmetric partial correlation matrix of 90×90 was obtained for each subject. Correlation between any two regions of interest reduced the indirect dependencies of the other 88 regions. When the time-series of two brain regions are highly correlated, it implies that the two regions are active at the same time. Using this approach, the mean correlation matrix for all subjects was computed. A sample processing procedure is shown in Figure 3.1.

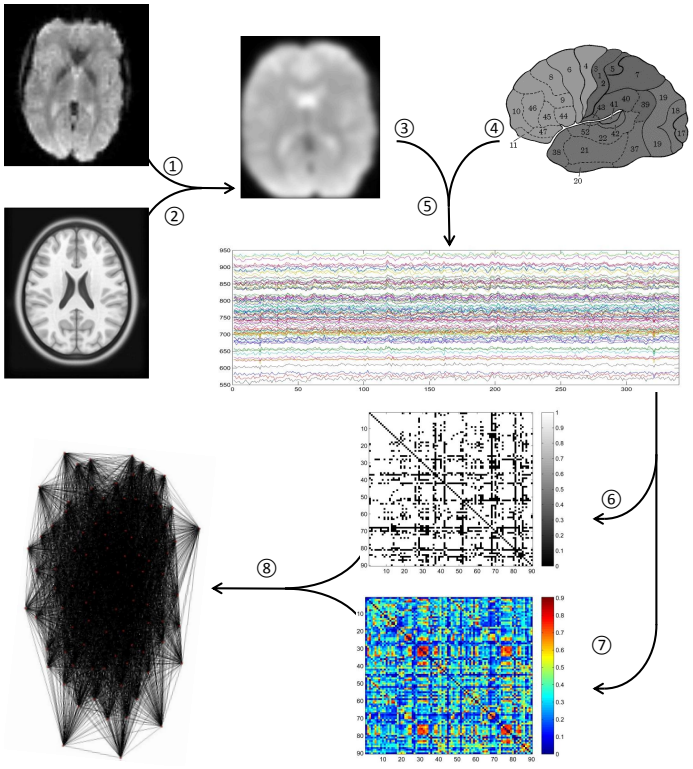

Figure 3.1: A flowchart for yielding brain connectivity data and network starts with functional (1) and anatomic (2) magnetic resonance imaging scans. In order to establish functional connectivity, a time series of brain activity in different voxels or regions can be derived. These images were later warped to the template (3) to register the location of brain regions. Once scans were registered, the brain regions were parcellated (4) according to the anatomical parcellation scheme described in [76] and 90 regional time series were extracted (5). In order to establish functional connectivity, time series of each brain region were derived and correlations between the time series of different voxels or brain regions were calculated and represented as a correlation matrix. The correlation matrix can be either directly interpreted as a binary network (6) or the weighted network (7). The weighted and binary network can be graphically represented by 3-dimensional connectivity network (8).

The individual partial correlation matrices were thresholded to ensure that each node in the network is not too densely clustered, nor too sparsely connected. In other words, thresholding was used in the study to eliminate the links that are likely to attenuate the effect of important connections [68]. The selection of threshold values significantly affected the topological properties of the

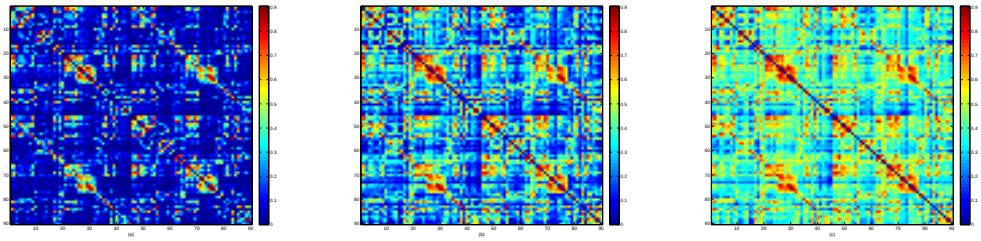

Figure 3.2: The effects of maintaining different node degrees on the connectivity matrix: (a) $K = 36$; (b) $K = 48$; and (c) $K = 60$.

thresholded networks, as different number of links in functional networks may represent a different magnitude of correlational interactions. Therefore, to ensure that the partial correlation matrix for each subject had the same number of links, we followed the method proposed by Supekar et al. [82]. Individual partial correlation matrices were thresholded such that each network after thresholding had on average K links per node. This approach ensured that both groups have the same number of links per node so that the topological properties of the networks were consistent. Moreover, we selected a conservative K to prevent the generated network from disconnect or containing non-significant connections. As shown in Figure 3.2, selecting 60 edges per node produced excessive connections while selecting 36 edges per node lost important connectivity information. Therefore, as suggested in [82], [42], we selected a K value equal to 48. All network constructed according to this approach had 2160 edges (=48$\times$90/2).

To understand the small-world properties of the obtained networks, the value of C and L from the functional network were compared with those of 1000 random networks generated by a Markov-chain algorithm [87]. In the random matrix generated by Markov-chain algorithm, if node i_1 was linked to j_1 and node i_2 was linked to j_2, then the link between node i_1 and j_1 was removed while a link between node i_2 and j_2 was added [32]. Then the matrix was randomly permuted such that the random matrix and original matrix had equivalent node degree. We repeated this procedure over $1,000$ random matrix generated by Markov-chain algorithm to obtain mean

C_{rand} and mean L_{rand} values for every degree and threshold value. In order to study the influence of thresholding, we calculated several network properties as a function of the sparsity thresholds. In order to calculate C_{rand} and L_{rand}, we followed the methodology outlined in [33].

In our study, we examined hierarchy values derived from both whole-brain functional networks and also swallowing related regions. These two connectivity matrices were constructed by thresholding the correlation matrix such that each node in the resulting network generally has 48 connections. The threshold values range from 0 to 1, with an increment of 0.05. In order to calculate hierarchy, the clustering coefficient C and node degree k had to be computed for every node in the network. In order to model the relationship between C and k, we fitted a fifth order linear regression curve to the express the relationship between $log(C)$ and $log(k)$.

3.5 COMPARISON BETWEEN THE WHOLE BRAIN AND SWALLOWING-RELATED REGIONS

In our analysis, we compared the network measures calculated for the whole brain and for the previously identified regions activated during swallowing (e.g., [50], [55], [56], [58]), which are listed in Table 3.2. We examined whether these network measures were affected by the selected regions.

3.6 NETWORK TOOLBOXES

In this study, we used an open source Brain Connectivity Toolbox (BCT) [68] for calculation of various network properties. The toolbox provides functions for a number of network measures. In addition, the toolbox enabled the network manipulation such as thresholding.

Table 3.2: Regions of brain activation associated with voluntary saliva swallowing. LH: Left Hemisphere. RH: Right Hemisphere.

Structure	Hemisphere	Structure	Hemisphere
Anterior cingulate and paracingulate gyri	LH/RH	Paracentral lobule	LH/RH
Median cingulate and paracingulate gyri	LH/RH	Inferior parietal, but supramarginal and angular gyri	LH/RH
Posterior cingulate gyrus	LH/RH	Superior parietal gyrus	LH/RH
Cuneus	LH/RH	Postcentral gyrus	LH
Middle frontal gyrus	LH/RH	Precentral gyrus	RH
Superior frontal gyrus, dorsolateral	LH/RH	Precuneus	LH/RH
Fusiform gyrus	LH	Lenticular nucleus, putamen	LH
Hippocampus	LH/RH	Supplementary motor area	LH/RH
Insula	LH/RH	Supramarginal gyrus	LH/RH
Lingual gyrus	LH/RH	Superior tempotal gyrus	LH/RH
Middle occipital gyrus	LH/RH	Thalamus	LH/RH
Superior occipital gyrus	LH/RH		

3.7 STATISTICAL TESTS

To distinguish the difference between swallowing related regions to whole brain metrics we used the non-parametric Mann-Whitney Wilcoxon rank-sum test [90].

4.0 RESULTS

Binary and weighted functional networks were created for all subjects using the outlined approach. These functional networks were sensitive to threshold values as shown in Figure 3.2, which depicts the effects of thresholding the partial correlation matrices such that each node in the resultant network had on average K connections. A summary of our results can be found below.

4.1 NETWORK FEATURES

As shown in Figure 4.1, significant differences in some of the network properties were found between the whole-brain matrices and swallowing related regions. No significant difference in node degree were observed between the two groups in the binary and weighted networks ($p > 0.29$).

However, global efficiency was higher when considering swallowing ROIs and sparsity threshold values lower than 0.35, but it did not reach statistical significance for all values ($p < 0.07$). The path length L of the binary and weighted network were significantly shorter in whole brain metric compared to swallowing related regions ($p < 0.05$) when the threshold value is within the range of 0.60 to 0.85. The local efficiency values were significantly higher when considering swallowing ROIs and threshold values within the range of 0 to 0.03 ($p < 0.05$). Interestingly, we found that clustering coefficient value has slightly increased when we apply threshold between 0.5 to 0.63. The rank-sum test showed that significant differences ($p < 0.05$) has been found within this interval between two comparison groups (i.e. Whole-Brain and Swallowing ROIs). Note that the differences in the clustering coefficient between the two comparison groups are even greater in this interval in comparison to low threshold values. This has never been found in other network

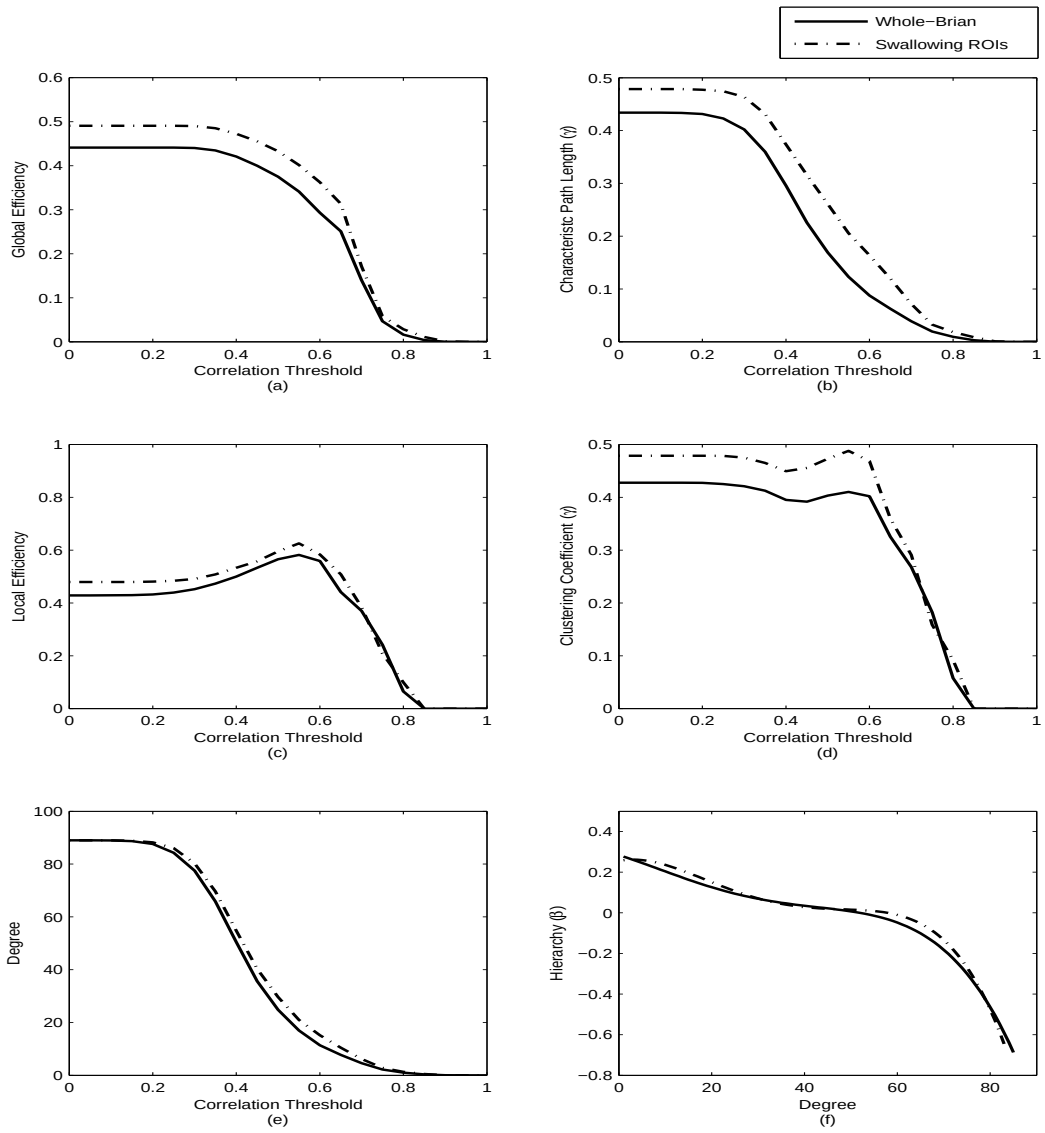

Figure 4.1: Comparison of networks measures for the swallowing ROIs and the whole brain: (a) global efficiency E_{global} (b) characteristic path length L_p (c) node degree K (d) clustering coefficient C (e) mean local efficiency E_{global} (f) hierarchy β.

measurement parameters. As shown in Figure 4.1 (f), the hierarchy values for swallowing ROIs and the whole brain were almost identical between two groups ($p > 0.45$).

Our study demonstrated the brain functional networks are characterized by small-world attributes. First of all, the mean network clustering coefficient C calculated was 0.45 and the mean minimum path length L was 0.32. Second, the parameters C and L for a random graph with same number of node, links and degree distribution were also calculated and the values were C_{rand} = 0.0116 and L_{rand} = 0.0119. From the above calculation, we observed that the ratio of local clustering of connections in the brain functional network over the random network was approximately 40, $\frac{C}{C_{rand}} = 38.71$, whereas the ratio of path length between any two brain regions in functional brain network random network was approximately 25, $\frac{L}{L_{rand}} = 26.93$.

4.2 INTER-REGIONAL FUNCTIONAL CONNECTIVITY

Figure 4.2 showed the mean map which was obtained by averaging across the weighted connectivity matrices of all 22 subjects (Table 3.1 showed the abbreviation corresponding to each ROI). The map is a 90$\times$ 90 symmetric matrix. These 90 regions were classified into six major locations as suggested by Salvador et al. [41]. Each entry in the map represented the percentage of the connectivity strength between the corresponding pair of regions. The value of each entry ranged from 0 (deep blue color in the map) to 1 (dark red color in the map), whereas 0 means no connection at all and 1 means that two corresponding regions are firmly connected. Network connections were also visualized by the Pajek software and the resulting connection map is shown in Figure 4.3.

As we can see in Figure 4.2, a lot of the connections were long-distance inter-hemispheric connections between bilaterally homologous brain regions. The uniqueness and importance of bilaterally symmetric inter-hemispheric connections can be highlighted in the study of functional network. One reason being that previous multivariate-analyses based brain anatomical network studies are uni-hemispheric, it limits the connections only within a single hemisphere, which are inter-regional connections with in left or right hemisphere [41].

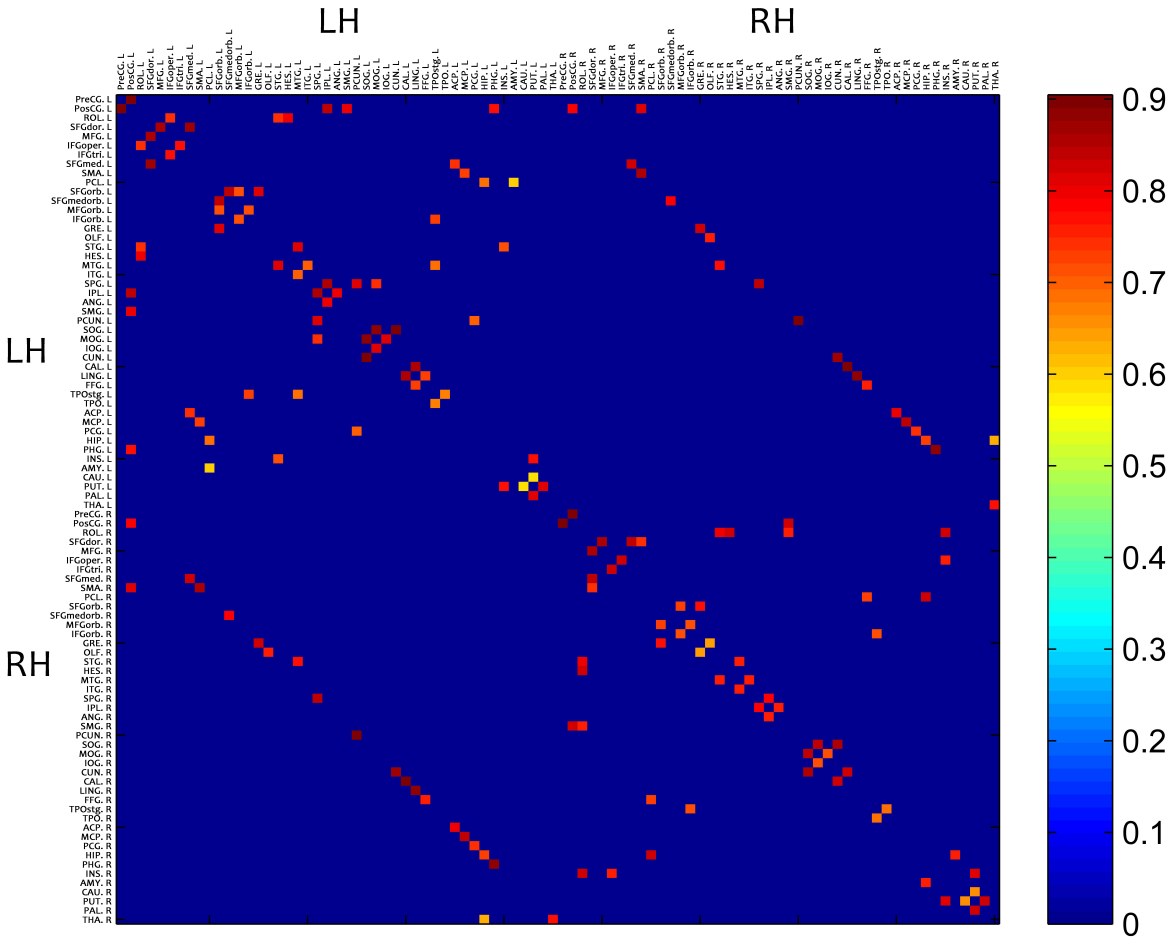

Figure 4.2: Mean map of the weighted connectivity matrixes averaged across the 22 subjects. LH: Left Hemisphere. RH: Right Hemisphere. (Refer to Table 3.2)

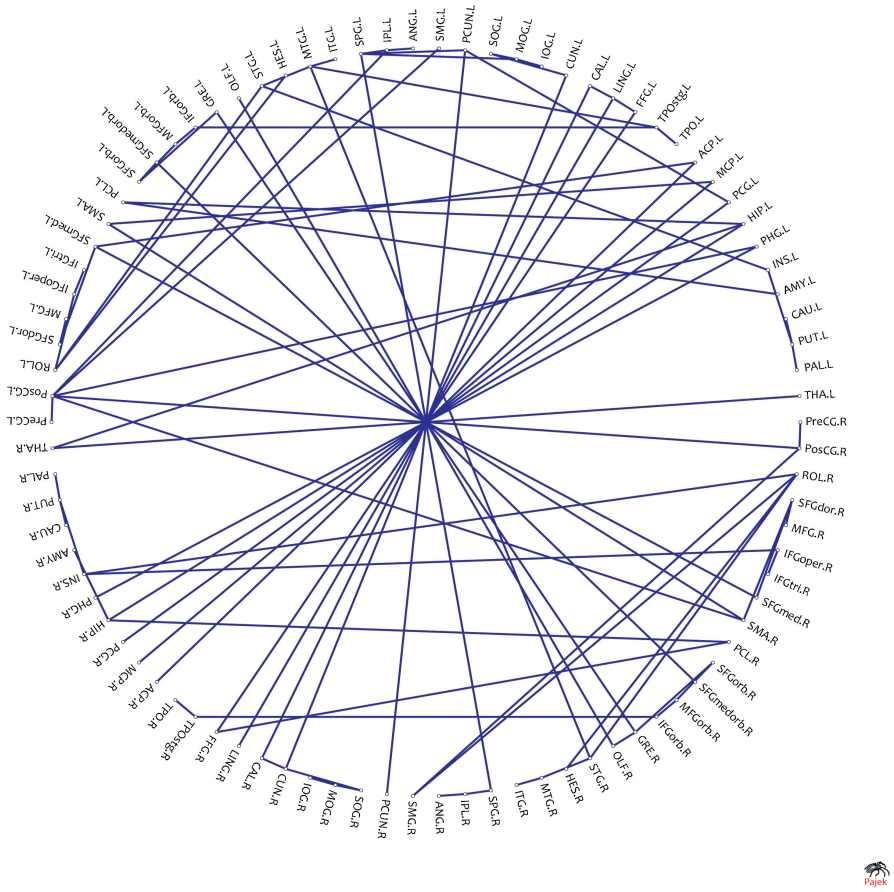

Figure 4.3: Mean map of the weighted connectivity matrixes averaged across the 22 subjects. LH: Left Hemisphere. RH: Right Hemisphere. (Refer to Table 3.2)

5.0 DISCUSSION

We believe that our study is the first one to use novel graph theoretical approaches to report brain functional connectivity during voluntary saliva swallowing. By utilizing the graph theoretical approaches, we are able to study the alteration of functional connectivity both at global as well as at the divisional scale.

Our results highlighted that the spatial topological connectivity in swallowing related regions are significantly distinguished compared to whole-brain properties, as can be reflected on various network measurement parameters. Furthermore, our results reported the advantage of applying functional connectivity analysis rather than anatomical connectivity analysis, which is the importance of bilaterally symmetric inter-hemispheric connections. This finding from functional connectivity during swallowing tasks has not been so clearly demonstrated by previous studies using anatomical connectivity approaches.

5.0.1 Network Measures

Network measures for weighted network in this study consist of characteristic path length (L), local efficiency (E_{loc}), global efficiency (E_{glob}), clustering coefficient (C), node degree (k), hierarchy (β), as well as the small-world attributes of the network (λ and γ). The average value of these network properties across all the 22 subjects were demonstrated in Figure 4.1. Also, small-world properties, although varying in some degree, were generally found in the weighted networks of every subject in the study. The small-world attributes and hierarchical organization for whole brain and swallowing ROIs are similar. However, global efficiency, characteristic path length, clustering coefficient and local efficiency shows higher value within the swallowing ROIs in comparison to the whole brain.

The characteristic path length was short in both whole-brain matrices and swallowing related regions, which indicates the distance between distinct brain regions are short during swallowing. Although both whole-brain matrices and swallowing related regions are showing low values, significant differences between these two groups were observed. We have observed that during swallowing the path lengths are significantly different in threshold interval from 0.60 to 0.85, which may suggest the threshold range to use when solely comparing characteristic path length for two different groups. The whole brain had a lower path length than swallowing related regions. This finding suggested that the entire brain functional network during swallowing consists of various short paths between nodes, which provides faster information transfer routes.

A clustering coefficient is defined as the proportion of the number of established connections in direct neighbors of the node to all their possible connections [61]. It can also denote the local efficiency of a network or the network's fault-tolerance [84]. Our study found that the whole brain values were lower in comparison to the values obtained for the swallowing related regions. To be more specific, we showed that the most significant differences were observed between threshold values 0.5 and 0.63 suggesting that more information was interpreted during swallowing.

Our study also reports small global efficiency values ($E_{glob} \sim 0.5$) compared to the random network ($E_{glob,rand} \sim 1$) although compared to other network measurements the difference is not phenomenal between two groups. The smaller E_{glob} values in functional brain networks compared to random networks showed that the functional brain networks are characterized by small-world properties indicated by [36]. In addition, higher global efficiency values in swallowing-related regions suggest optimal information transfer efficiency of swallowing-related regions in comparison to the whole brain.

5.0.2 Small-Worldness

Our study revealed that the brain functional network associated with swallowing is a large complex network with efficient small-world properties. The small-world parameters calculated for this study are consistent with small-world attributes for brain functional network. This further implies that distinct small-world properties was generally found in the weighted networks of every subject

in the study. As we have calculated, the clustering coefficient in the brain network was generally 40 times larger than in the random network. That is to say, the brain network is about forty times as clustered as to a random network. Also, between any two brain regions in the network, the path length was approximately twenty times longer compared to the random network. A higher absolute clustering coefficient and shorter absolute path length in the functional brain network suggests an optimal small-world profile [42], which benefits the local segregation and global integration within the brain functional network [33].

5.0.3 Inter-Regional Functional Connectivity

The average functional brain network, shown in Figure 4.2, primarily consisted of strong connections between closely neighboring brain regions. This demonstrated that anatomically related regions are also likely to be functionally connected. However, functionally connected regions do not necessarily have anatomical connections. Other than intra-hemispheric connections, our data highlighted the bilaterally homologous long-range connections (e.g. PHG.L to PHG.R., SFGmed.L to SFGmed.R,SMA.L to SMA.R and etc). These inter-hemispheric connections are strong in connectivity strength ($w_{ij} > 0.55$) and have not been previously reported according to their anatomical distances [72], which clearly shows the advantage of performing functional network analysis to human brain networks. The importance of bilaterally symmetric inter-hemispheric connections can be highlighted in the study of functional networks. One reason being that previous anatomical connectivity studies on which multivariate analyses have been based are uni-hemispheric, it summarize inter-regional connections only within a single (right or left) hemisphere [41]. In addition to inter-hemispheric homologus connections, our results demonstrated few non-symmetrical bilaterally inter-hemispheric connections that also have not been reported before, such as SMA.R to PosCG.L, STG.R to HES.L, etc, as shown in Figure 4.2. These connections are strongly correlated ($w_{ij} > 0.70$) during swallowing tasks.

Compare to previous functional network studies on various tasks, the functional networks during swallowing shows some unique connections. Wang et at. [29] performed functional connectivity analysis during memory encoding and recognition tasks. Their study showed strong functional

connectivity between anatomical adjacent regions. However, the bilaterally homologous long-range connections show relatively low connectivity strength ($w_{ij} < 0.25$), neither did the unique connections (PosCG.L to SMA.R, HIP.L to THA.R) exist in this study. We also referred to other functional connectivity studies [82], [42], neither of the studies has shown bilaterally homologous long-range connections, which further convinced us the unique connectivity pattern during swallowing.

Also, the higher degree and stronger strength of functional connectivity in swallowing ROIs (as can be seen in Figure 4.2) not only demonstrated a more densely connected network during swallowing, but also indicate an increased activation of functionally related brain regions during swallowing.

Correlation between swallowing related regions in the functional connectivity matrices suggests that this approach could be helpful in understanding the inner connections among regions during swallowing. This approach can also be used as a visualization tool of functional connectivity.

6.0 CONCLUSION AND FUTURE WORK

6.1 CONCLUSION

In this study, we successfully reconstructed the weighted functional networks during swallowing based on fMRI recordings from 22 subjects. We utilized graph theoretical approaches to produce a set of measures that quantified properties for swallowing related ROIs and whole brain metrics of a brain functional network. The main findings in the study were: (1) Swallowing regions and the whole brain metrics showed a similar node degree distribution and optimal small-world properties. (2) Swallowing related areas had distinct inter-regional connectivity patterns. (3) The network properties of large-scale brain connectivity differs significantly between swallowing related areas and the whole brain. Collectively, these and other findings reported in this study provided new insights into how graph theoretical approaches can be utilized to describe the brain functional network during swallowing and thus provided new clues for understanding the mechanism of swallowing.

6.2 FUTURE WORK

The rising field of complex brain networks provides insight into topolocial properties of human brain network architecture and also raises a number of interesting questions for future. An important focus for future research efforts is how the parameters of the complex network measurements relate to the swallowing functions. From our current study, we can only make an intuitively conclusion that high clustering coefficient indicates locally specialized information processing while short path length suggest information processing at a relatively low cost. However, there is no solid theory to support such an empirical guess. This will probably be a important concentration of our future work.

Second, a large number of previous studies has shown that brain activation during swallowing is affected by different type of fluids [49], [50], [51], [52], [53], [54], [55], [56], [57], but that not all types of fluid affect the network property equally. Therefore, it would be worthwhile to utilize other varieties of fluids (e.g. water, nector-thick juice and honey-thick juice), in order to examine whether they display similar network properties.

Furthermore, our current study also contains certain limitations. The sample size employed in this study was relatively small, which may have partially contributed to the non-significant correlation between network parameter and performance mentioned above. In future studies, a larger sample would be vital to provide the statistical power necessary to validate these findings.

BIBLIOGRAPHY

[1] W. J. Dodds, E. T. Stewart, and J. A. Logemann, "Physiology and radiology of the normal oral and pharyngeal phases of swallowing." *American Journal of Roentgenology*, vol. 154, no. 5, pp. 953–963, 1990.

[2] C. Ertekin and I. Aydogdu, "Neurophysiology of swallowing," *Clinical Neurophysiology*, vol. 114, no. 12, pp. 2226 – 2244, 2003.

[3] R. D. Stevenson, J. H. Allaire *et al.*, "The development of normal feeding and swallowing." *Pediatric Clinics of North America*, vol. 38, no. 6, p. 1439, 1991.

[4] A. J. Miller, *The neuroscientific principles of swallowing and dysphagia*. Singular Publishing Group San Diego; London, 1999.

[5] N. H. Bass and R. M. Morrell, "The neurology of swallowing," *Dysphagia–diagnosis and management. 3rd ed. Boston: Butterworth–Heinemann*, pp. 7–35, 1997.

[6] A. Miller, "Deglutition." *Physiological Reviews*, vol. 62, no. 1, pp. 129–184, 1982, cited By (since 1996) 247.

[7] A. Jean, "Brainstem organization of the swallowing network," *Brain, behavior and evolution*, vol. 25, no. 2-3, pp. 109–116, 1984.

[8] ——, "Control of the central swallowing program by inputs from the peripheral receptors. a review," *Journal of the autonomic nervous system*, vol. 10, no. 3, pp. 225–233, 1984.

[9] ——, "Brain stem control of swallowing: neuronal network and cellular mechanisms," *Physiological Reviews*, vol. 81, no. 2, pp. 929–969, 2001.

[10] M. W. Donner, J. F. Bosnia, and D. L. Robertson, "Anatomy and physiology of the pharynx," *Abdominal Imaging*, vol. 10, no. 1, pp. 197–212, 1985.

[11] D. L. Broussard and S. M. Altschuler, "Central integration of swallow and airway-protective reflexes," *The American journal of medicine*, vol. 108, no. 4, pp. 62–67, 2000.

[12] C. M. Wiles, "The neuroscientific principles of swallowing and dysphagia." *Brain*, vol. 122, no. 4, pp. 788–789, 1999.

[13] E. Mbonda, D. Claus, C. Bonnier, P. Evrard, J. Gadisseux, and G. Lyon, "Prolonged dysphagia caused by congenital pharyngeal dysfunction," *The Journal of Pediatrics*, vol. 126, no. 6, pp. 923 – 927, 1995.

[14] L. L. Riensche and K. Lang, "Treatment of swallowing disorders through a multidisciplinary team approach," *Educational Gerontology*, vol. 18, no. 3, pp. 277–284, 1992.

[15] J. Curran, "Nutritional considerations," *Dysphagia: diagnosis and management*, pp. 255–266, 1992.

[16] D. Smithard, P. O'Neill, C. Park, J. Morris, R. Wyatt, R. England, and D. Martin, "Complications and outcome after acute stroke: Does dysphagia matter?" *Stroke*, vol. 27, no. 7, pp. 1200–1204, 1996.

[17] E. Sejdic, C. Steele, and T. Chau, "Segmentation of dual-axis swallowing accelerometry signals in healthy subjects with analysis of anthropometric effects on duration of swallowing activities," *Biomedical Engineering, IEEE Transactions on*, vol. 56, no. 4, pp. 1090–1097, april 2009.

[18] J. A. Logemann and J. A. Logemann, "Evaluation and treatment of swallowing disorders," 1983.

[19] A. Tabaee, P. E. Johnson, C. J. Gartner, K. Kalwerisky, R. B. Desloge, and M. G. Stewart, "Patient-controlled comparison of flexible endoscopic evaluation of swallowing with sensory testing (feesst) and videofluoroscopy," *The Laryngoscope*, vol. 116, no. 5, pp. 821–825, 2006.

[20] C. Steele, C. Allen, J. Barker, P. Buen, R. French, A. Fedorak, S. Day, J. Lapointe, L. Lewis, C. MacKnight *et al.*, "Dysphagia service delivery by speech-language pathologists in canada: results of a national survey," *Canadian Journal of Speech-Language Pathology and Audiology*, vol. 31, no. 4, pp. 166–177, 2007.

[21] B. Sherman, J. M. Nisenboum, B. L. Jesberger, C. A. Morrow, and J. A. Jesberger, "Assessment of dysphagia with the use of pulse oximetry," *Dysphagia*, vol. 14, no. 3, pp. 152–156, 1999.

[22] P. Leslie, M. J. Drinnan, P. Finn, G. A. Ford, and J. A. Wilson, "Reliability and validity of cervical auscultation: a controlled comparison using videofluoroscopy," *Dysphagia*, vol. 19, no. 4, pp. 231–240, 2004.

[23] C. Ertekin, I. Aydogdu, N. Yüceyar, S. Tarlaci, N. Kiylioglu, M. Pehlivan, and G. Çelebi, "Electrodiagnostic methods for neurogenic dysphagia," *Electroencephalography and Clinical Neurophysiology/Electromyography and Motor Control*, vol. 109, no. 4, pp. 331–340, 1998.

[24] A. Das, N. P. Reddy, and J. Narayanan, "Hybrid fuzzy logic committee neural networks for recognition of swallow acceleration signals," *Computer Methods and Programs in Biomedicine*, vol. 64, no. 2, pp. 87–99, 2001.

[25] J. Lee, C. Steele, and T. Chau, "Time and time–frequency characterization of dual-axis swallowing accelerometry signals," *Physiological measurement*, vol. 29, no. 9, p. 1105, 2008.

[26] J. Lee, S. Blain, M. Casas, D. Kenny, G. Berall, and T. Chau, "A radial basis classifier for the automatic detection of aspiration in children with dysphagia," *Journal of NeuroEngineering and Rehabilitation*, vol. 3, no. 1, p. 14, 2006.

[27] E. Sejdić, T. H. Falk, C. M. Steele, and T. Chau, "Vocalization removal for improved automatic segmentation of dual-axis swallowing accelerometry signals," *Medical engineering & physics*, vol. 32, no. 6, pp. 668–672, 2010.

[28] H. Kashima and W. Berg, "Upper digestive tract evaluation and imaging," *Byron J. Bailey's Head & Neck Surgery-Otolaryngology, Third Edition, Lippincott & Wilkins, Philadelphia*, pp. 489–495, 2001.

[29] L. Wang, Y. Li, P. Metzak, Y. He, and T. S. Woodward, "Age-related changes in topological patterns of large-scale brain functional networks during memory encoding and recognition," *NeuroImage*, vol. 50, no. 3, pp. 862–872, 2010.

[30] S. Achard, R. Salvador, B. Whitcher, J. Suckling, and E. Bullmore, "A resilient, low-frequency, small-world human brain functional network with highly connected association cortical hubs," *The Journal of Neuroscience*, vol. 26, no. 1, pp. 63–72, 2006.

[31] Y. Liu, M. Liang, Y. Zhou, Y. He, Y. Hao, M. Song, C. Yu, H. Liu, Z. Liu, and T. Jiang, "Disrupted small-world networks in schizophrenia," *Brain*, vol. 131, no. 4, pp. 945–961, 2008.

[32] W. Liao, Z. Zhang, Z. Pan, D. Mantini, J. Ding, X. Duan, C. Luo, G. Lu, and H. Chen, "Altered functional connectivity and small-world in mesial temporal lobe epilepsy," *PLoS One*, vol. 5, no. 1, p. e8525, 2010.

[33] Y. Liu, M. Liang, Y. Zhou, Y. He, Y. Hao, M. Song, C. Yu, H. Liu, Z. Liu, and T. Jiang, "Disrupted small-world networks in schizophrenia," *Brain*, vol. 131, no. 4, pp. 945–961, 2008.

[34] O. Sporns, D. R. Chialvo, M. Kaiser, and C. C. Hilgetag, "Organization, development and function of complex brain networks," *Trends in Cognitive Sciences*, vol. 8, no. 9, pp. 418–425, 2004.

[35] Y. Iturria-Medina, R. C. Sotero, E. J. Canales-Rodrguez, Y. Alemn-Gmez, and L. Melie-Garca, "Studying the human brain anatomical network via diffusion-weighted MRI and graph theory," *NeuroImage*, vol. 40, no. 3, pp. 1064–1076, 2008.

[36] D. J. Watts and S. H. Strogatz, "Collective dynamics of 'small-world' networks," *Nature*, vol. 393, pp. 440–442, June 1998.

[37] L. Ferrarini, I. M. Veer, E. Baerends, M.-J. van Tol, R. J. Renken, N. J. van der Wee, D. J. Veltman, A. Aleman, F. G. Zitman, B. W. Penninx *et al.*, "Hierarchical functional modularity in the resting-state human brain," *Human brain mapping*, vol. 30, no. 7, pp. 2220–2231, 2009.

[38] B. M. Unit, "Age-related changes in modular organization of human brain functional networks," *Neuroimage*, vol. 44, pp. 715–723, 2009.

[39] R. Riedl, M. Hubert, and P. Kenning, "Are there neural gender differences in online trust? an fmri study on the perceived trustworthiness of ebay offers," *MIS Quarterly*, vol. 34, no. 2, pp. 397–428, 2010.

[40] A. O. Ceballos-Baumann, "Functional imaging in parkinson's disease: activation studies with pet, fmri and spect," *Journal of neurology*, vol. 250, pp. 15–23, 2003.

[41] R. Salvador, J. Suckling, M. R. Coleman, J. D. Pickard, D. Menon, and E. Bullmore, "Neurophysiological architecture of functional magnetic resonance images of human brain," *Cerebral Cortex*, vol. 15, no. 9, pp. 1332–1342, September 2005.

[42] K. Supekar, V. Menon, D. Rubin, M. Musen, and M. D. Greicius, "Network analysis of intrinsic functional brain connectivity in alzheimer's disease," *PLoS Computational Biology*, vol. 4, no. 6, pp. e1 000 100–1–11, 2008.

[43] P. J. Planetta, J. Prodoehl, D. M. Corcos, and D. E. Vaillancourt, "Use of mri to monitor parkinson's disease," *Neurodegenerative Disease Management*, vol. 1, no. 1, pp. 67–77, 2011.

[44] R. D. Terry, E. Masliah, D. P. Salmon, N. Butters, R. DeTeresa, R. Hill, L. A. Hansen, and R. Katzman, "Physical basis of cognitive alterations in alzheimer's disease: synapse loss is the major correlate of cognitive impairment," *Annals of neurology*, vol. 30, no. 4, pp. 572–580, 2004.

[45] L. Wang, Y. Zang, Y. He, M. Liang, X. Zhang, L. Tian, T. Wu, T. Jiang, K. Li *et al.*, "Changes in hippocampal connectivity in the early stages of alzheimer's disease: evidence from resting state fmri," *Neuroimage*, vol. 31, no. 2, pp. 496–504, 2006.

[46] S. P. H. J. Nestor, P.J., "Adance in the early detection of alzheimers disease." *Nature Reviews Neuroscience*, vol. 5, pp. 34–41, 2004.

[47] B. T. Hyman, G. W. Van Hoesen, A. R. Damasio, C. L. Barnes *et al.*, "Alzheimer's disease: cell-specific pathology isolates the hippocampal formation." *Science (New York, NY)*, vol. 225, no. 4667, p. 1168, 1984.

[48] B. Hyman, G. Van Hoesen, L. Kromer, and A. Damasio, "Perforant pathway changes and the memory impairment of alzheimer's disease," *Annals of neurology*, vol. 20, no. 4, pp. 472–481, 2004.

[49] S. Hamdy, D. J. Mikulis, A. Crawley, S. Xue, H. Lau, S. Henry, and N. E. Diamant, "Cortical activation during human volitional swallowing: an event-related fmri study," *American Journal of Physiology - Gastrointestinal and Liver Physiology*, vol. 277, no. 1, pp. G219–1–G225–7, 1999.

[50] M. K. Kern, S. Jaradeh, R. C. Arndorfer, and R. Shaker, "Cerebral cortical representation of reflexive and volitional swallowing in humans," *American Journal of Physiology - Gastrointestinal and Liver Physiology*, vol. 280, no. 3, pp. G354–1–G360–7, 2001.

[51] R. Dziewas, P. Sörös, R. Ishii, W. Chau, H. Henningsen, E. B. Ringelstein, S. Knecht, and C. Pantev, "Neuroimaging evidence for cortical involvement in the preparation and in the act of swallowing," *NeuroImage*, vol. 20, no. 1, pp. 135–144, 2003.

[52] R. E. Martin, B. J. MacIntosh, R. C. Smith, A. M. Barr, T. K. Stevens, J. S. Gati, and R. S. Menon, "Cerebral areas processing swallowing and tongue movement are overlapping but distinct: A functional magnetic resonance imaging study," *Journal of Neurophysiology*, vol. 92, no. 4, pp. 2428–2493, 2004.

[53] R. Martin, A. Barr, B. MacIntosh, R. Smith, T. Stevens, D. Taves, J. Gati, R. Menon, and V. Hachinski, "Cerebral cortical processing of swallowing in older adults," *Experimental Brain Research*, vol. 176, pp. 12–22, 2007.

[54] S. Y. Lowell, C. J. Poletto, B. R. Knorr-Chung, R. C. Reynolds, K. Simonyan, and C. L. Ludlow, "Sensory stimulation activates both motor and sensory components of the swallowing system," *NeuroImage*, vol. 42, no. 1, pp. 285–295, 2008.

[55] R. E. Martin, B. G. Goodyear, J. S. Gati, and R. S. Menon, "Cerebral cortical representation of automatic and volitional swallowing in humans," *Journal of Neurophysiology*, vol. 85, no. 2, pp. 938–950, 2001.

[56] K. M. Mosier, W.-C. Liu, J. A. Maldjian, R. Shah, and B. Modi, "Lateralization of cortical function in swallowing: A functional mr imaging study," *American Journal of Neuroradiology*, vol. 20, no. 8, pp. 1520–1526, 1999.

[57] D. H. Zald and J. V. Pardo, "The functional neuroanatomy of voluntary swallowing," *Annals of Neurology*, vol. 46, no. 3, pp. 281–286, 1999.

[58] P. Sörös, Y. Inamoto, and R. E. Martin, "Functional brain imaging of swallowing: an activation likelihood estimation meta-analysis." *Human Brain Mapping*, vol. 30, no. 8, pp. 2426–39, 2009.

[59] P. Sörös, F. Al-Otaibi, S. W. H. Wong, J. K. Shoemaker, S. M. Mirsattari, V. Hachinski, and R. E. Martin, "Stuttered swallowing: Electric stimulation of the right insula interferes with water swallowing. a case report," *BMC Neurology*, vol. 11, no. 1, p. 20, 2011.

[60] O. Sporns and J. Zwi, "The small world of the cerebral cortex," *Neuroinformatics*, vol. 2, pp. 145–162, 2004.

[61] M. Kaiser, "A tutorial in connectome analysis: Topological and spatial features of brain networks," *NeuroImage*, vol. 57, no. 3, pp. 892–907, 2011.

[62] J. Cameron, J. Reynolds, G. Zuidema *et al.*, "Aspiration in patients with tracheostomies," *Surg Gynecol Obstet*, vol. 136, no. 1, pp. 68–70, 1973.

[63] A. J. Miller, "Deglutition." *Physiological Reviews*, vol. 62, no. 1, pp. 129–184, 1982.

[64] [Online]. Available: http://www.nestlenutrition.co.uk/healthcare/gb/health_concerns/dysphagia/pages/dymechanismofdysphagia.aspx

[65] R. W. Doty and J. F. Bosma, "An electromyographic analysis of reflex deglutition." *Journal of Neurophysiology*, 1956.

[66] R. W. Doty, W. H. Richmond, and A. T. Storey, "Effect of medullary lesions on coordination of deglutition," *Experimental neurology*, vol. 17, no. 1, pp. 91–106, 1967.

[67] E. Bullmore and O. Sporns, "Complex brain networks: graph theoretical analysis of structural and functional systems," *Nature Reviews Neuroscience*, vol. 10, pp. 186–198, 2009.

[68] M. Rubinov and O. Sporns, "Complex network measures of brain connectivity: Uses and interpretations," *NeuroImage*, vol. 52, no. 3, pp. 1059–1069, 2010.

[69] B. Horwitz *et al.*, "The elusive concept of brain connectivity," *Neuroimage*, vol. 19, no. 2, pp. 466–470, 2003.

[70] A. A. Ioannides, "Dynamic functional connectivity," *Current opinion in neurobiology*, vol. 17, no. 2, pp. 161–170, 2007.

[71] [Online]. Available: http://en.wikipedia.org/wiki/Graph_(mathematics)

[72] Y. Li, Y. Liu, J. Li, W. Qin, K. Li, C. Yu, and T. Jiang, "Brain anatomical network and intelligence," *PLOS Computational Biology*, vol. 5, no. 5, pp. e1 000 395–1–17, 2009.

[73] K. Friston, 2005. [Online]. Available: http://www.fil.ion.ucl.ac.uk/spm/

[74] K. Friston, C. Frith, R. Frackowiak, and R. Turner, "Characterizing dynamic brain responses with fmri: A multivariate approach," *NeuroImage*, vol. 2, no. 2, Part A, pp. 166–172, 1995.

[75] L.-L. Zeng, H. Shen, L. Liu, L. Wang, B. Li, P. Fang, Z. Zhou, Y. Li, and D. Hu, "Identifying major depression using whole-brain functional connectivity: a multivariate pattern analysis," *Brain*, vol. 135, no. 5, pp. 1498–1507, 2012.

[76] N. Tzourio-Mazoyer, B. Landeau, D. Papathanassiou, F. Crivello, O. Etard, N. Delcroix, B. Mazoyer, and M. Joliot, "Automated anatomical labeling of activations in spm using a macroscopic anatomical parcellation of the mni mri single-subject brain," *NeuroImage*, vol. 15, no. 1, pp. 273–289, 2002.

[77] M. Brett, J.-L. Anton, R. Valabregue, and J.-B. Poline, "Region of interest analysis using an SPM toolbox," in *8th International Conference on Functional Mapping of the Human Brain*, Sendai, Japan, Jun. 2-6 2002.

[78] A.-L. Barabasi, R. Albert, and H. Jeong, "Scale-free characteristics of random networks: the topology of the world-wide web," *Physica A: Statistical Mechanics and its Applications*, vol. 281, no. 14, pp. 69–77, 2000.

[79] S. Boccaletti, V. Latora, Y. Moreno, M. Chavez, and D.-U. Hwang, "Complex networks: Structure and dynamics," *Physics Reports*, vol. 424, no. 45, pp. 175–308, 2006.

[80] V. Latora and M. Marchiori, "Efficient behavior of small-world networks," *Physical Review Letters*, vol. 87, pp. 198 701–1–4, 2001.

[81] S. Achard and E. Bullmore, "Efficiency and cost of economical brain functional networks," *PLoS Computational Biology*, vol. 3, no. 2, pp. e17–0174–0183, 02 2007.

[82] K. Supekar, M. Musen, and V. Menon, "Development of large-scale functional brain networks in children," *PLoS Biology*, vol. 7, no. 7, pp. e1 000 157–1–15, 2009.

[83] M. E. J. Newman, "The structure and function of complex networks," *SIAM Review*, vol. 45, no. 2, pp. 167–256, 2003.

[84] S. H. Strogatz, "Exploring complex networks." *Nature*, no. 410, pp. 268–276, 2001.

[85] G. Gong, Y. He, L. Concha, C. Lebel, D. W. Gross, A. C. Evans, and C. Beaulieu, "Mapping anatomical connectivity patterns of human cerebral cortex using in vivo diffusion tensor imaging tractography," vol. 19, no. 3, pp. 524–536, 2009.

[86] D. S. Bassett, E. Bullmore, B. A. Verchinski, V. S. Mattay, D. R. Weinberger, and A. Meyer-Lindenberg, "Hierarchical organization of human cortical networks in health and schizophrenia," *The Journal of Neuroscience*, vol. 28, no. 37, pp. 9239–9248, 2008.

[87] E. Ravasz and A.-L. Barabási, "Hierarchical organization in complex networks," *Physical Review E*, vol. 67, pp. 026 112–1–7, 2003.

[88] C. J. Honey, O. Sporns, L. Cammoun, X. Gigandet, J. P. Thiran, R. Meuli, and P. Hagmann, "Predicting human resting-state functional connectivity from structural connectivity," *Proceedings of the National Academy of Sciences*, vol. 106, no. 6, pp. 2035–2040, 2009.

[89] J. Whittaker, "Graphical models in applied multivariate statistics," *Journal of Classification*, vol. 9, pp. 159–160, 1992.

[90] H. B. Mann and D. R. Whitney, "On a test of whether one of two random variables is stochastically larger than the other," *Analysis of Mathematical Statistics*, vol. 18, no. 1, pp. 50–60, 1947.